Application note

Automated particle analysis of Nb-V-rich precipitates in microalloyed steel

Authors
Alice Scarpellini, Helen Oppong-Mensah, and Marc Liu, Thermo Fisher Scientific

Microalloyed and high-strength low-alloy (HSLA) steels are widely used in demanding applications, including structural construction and heavy equipment, where strength, toughness, and reliable processability are required.

In these materials, niobium and vanadium are commonly added in small amounts to support microstructural control and improve mechanical performance. Their effect is linked to the formation of microalloyed precipitates, which can contribute to grain refinement, control of recrystallization, and precipitation strengthening, depending on the steel composition, particle chemistry, and processing route (Lu-yan Sun, 2022).

The value of these precipitates depends not only on their presence but also on their chemistry, size, abundance, and distribution within the steel. Mixed precipitates that contain Nb and V have been reported in microalloyed steels and are commonly interpreted as complex carbide or carbonitride particles. Their metallurgical value is linked to their ability to contribute to microstructural control, particularly when they are fine and well distributed (Hardy Mohrbacher, 2023).

Characterizing these precipitates can help assess whether the material shows the intended characteristics and supports comparison between different batches or processing conditions. Particle analysis workflows are therefore of particular interest because they make it possible to statistically and repeatably evaluate precipitate populations.

Materials and characterization challenges

The material investigated here is a microalloyed steel that contains Nb-rich precipitates. Because these precipitates can be very small, characterizing them requires statistically meaningful datasets as well as sufficient spatial resolution to detect the fine particle population.

High-resolution techniques such as transmission electron microscopy (TEM) and scanning transmission electron microscopy (STEM) are well suited to the smallest precipitates, but they are less practical for routine, high-throughput screening over larger areas. Scanning electron microscopy (SEM)-based analysis is more accessible for automated, large-area characterization.

However, the smallest precipitates may approach the practical limits of detection and classification with SEM and energy-dispersive X-ray spectroscopy (EDS).

This creates a need for automated approaches that combine statistical particle analysis with the imaging and analytical capability required to detect smaller precipitates.

This application note demonstrates such an approach using Thermo Scientific™ Perception Software on the Thermo Scientific™ Apreo ChemiSEM™ System.

Integrated and automated precipitate analysis: Apreo ChemiSEM System and Perception Software

In the presented workflow, Perception Software was used to perform particle analysis of the Nb-V-rich precipitate population. Perception Software offers automated morphology and EDS data collection, particle classification based on morphology and EDS information, and customizable classification rules. In this application, these capabilities were used to detect candidate particles, classify particles containing Nb and V, and generate a statistical description of the precipitate population.

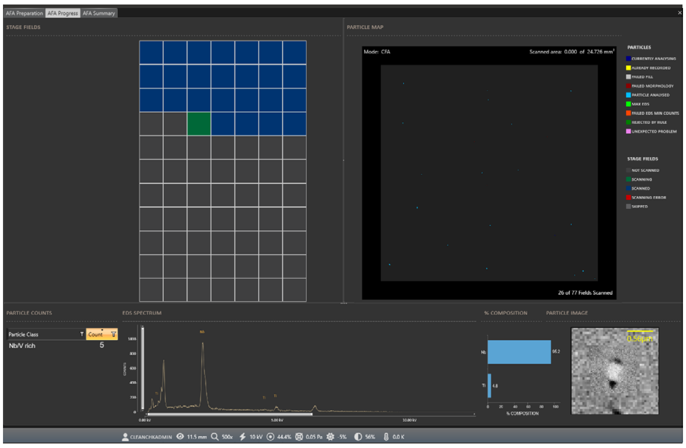

Figure 1. Live Perception Software overview during automated SEM-EDS particle analysis. The interface shows the acquired stage fields, classified particle count, and live information from the currently detected particle, including its EDS spectrum, composition, and image.

Candidate particles were detected from SEM images and analyzed with EDS. Particles that met the defined chemistry-based criteria were assigned to the Nb-V-rich precipitate class, allowing the analysis to focus on the target particle population while separating it from the surrounding Fe-rich matrix and other non-target features. Because the classification is based on SEM-EDS chemistry, the detected particles are described as Nb-V-rich precipitates rather than assigned to a specific carbide or carbonitride phase.

The automated particle analysis was performed at 10 kV to balance X-ray signal generation with spatial resolution. Compared with higher accelerating voltages, using lower voltages reduces the interaction volume and can improve localization of the signal from small particles. This is particularly relevant for Nb-rich precipitates embedded in an Fe-rich matrix, where the measured spectrum may include contributions from the surrounding steel matrix.

During method development, the particle-detection and classification parameters were adjusted to improve detection of small Nb-rich precipitate populations while limiting contribution from the surrounding steel matrix and other non-target features. Under the selected conditions, the automated run produced a sparse but clearly measurable population of classified Nb-rich particles, with particle densities on the order of several hundred particles per mm^2. This value should not be treated as an intrinsic material constant because the abundance of Nb-, V-, and mixed microalloyed precipitates depends on alloy composition and thermal history (Hardy Mohrbacher, 2023).

The generated dataset links each classified particle to its position in the analyzed area, measured dimensions, classification, particle image, segmentation mask, and EDS spectrum. This allows the results to be reviewed at both the population level and the single-particle level (see Figure 2).

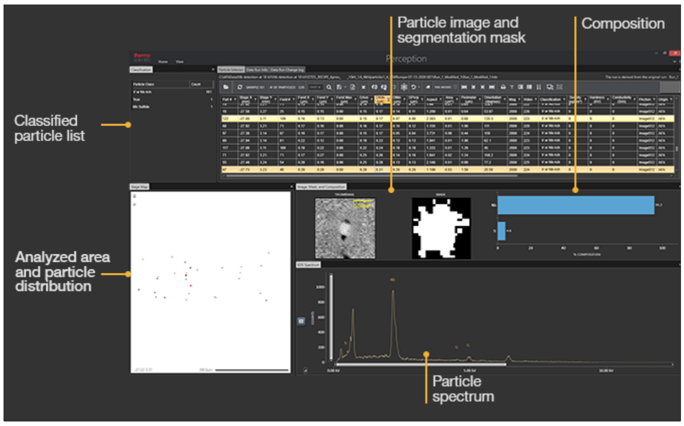

Figure 2. The results view in Perception Software links the classified particle list with the analyzed area, particle distribution, particle image, segmentation mask, EDS-based composition, and spectrum.

Representative examples from the same run, presented in Figure 3, illustrate the approximate size range of the classified population, including particles in the lower-hundreds-of-nanometers range and larger features approaching 2 µm. These examples are shown to demonstrate the range of particles captured under the selected analysis conditions, not to define the absolute detection limit of the method.

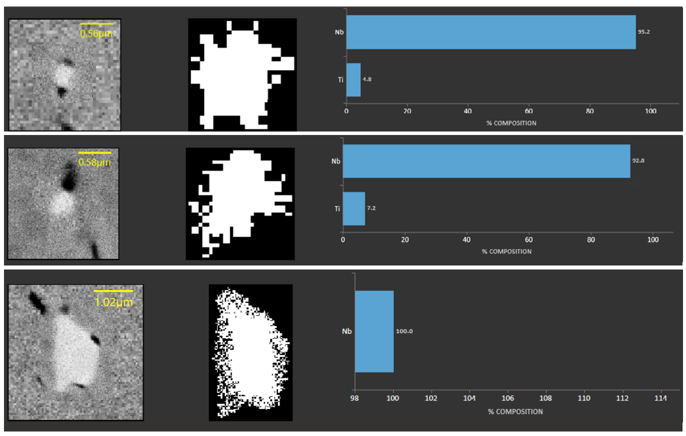

Figure 3. Representative Nb-rich candidate particles detected during automated SEM-EDS analysis. The particle image, segmentation mask, and EDS-based composition are shown for selected classified particles.

Overall, the results demonstrate the potential of the automated SEM-EDS workflow to identify and classify Nb-rich candidate particles in the sub-micrometer range. Further refinement of the detection and classification parameters may increase sensitivity toward smaller particles and improve separation of the target precipitate population from other microstructural features.

Complementary microstructure characterization with ChemiSEM Technology and the TruePix EBSD Detector

Perception Software provides a statistical and traceable description of the targeted Nb-rich particle population. To place these particles in their metallurgical context, Thermo Scientific™ ChemiSEM™ Technology and the Thermo Scientific™ TruePix EBSD Detector were used to inspect selected regions in greater detail and characterize the surrounding steel matrix. Together, these techniques support the interpretation of the detected Nb-rich particles in relation to the surrounding microstructure.

ChemiPhase, the phase-mapping component available within ChemiSEM Technology, was used to provide a more detailed understanding of the matrix surrounding the precipitates. ChemiPhase is based on multivariate statistical analysis applied to the EDS dataset: pixels with similar spectral signatures are grouped to generate composition-based phase maps.

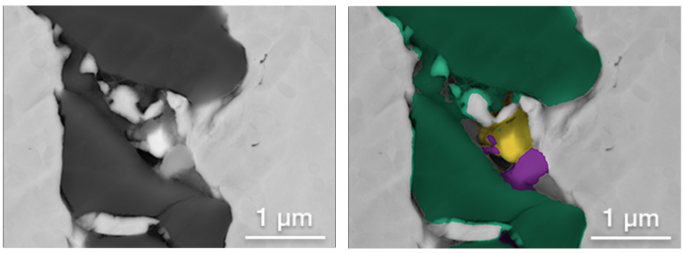

Figure 4. BSE and ChemiPhase images show the different inclusions and precipitates identified in the area of interest. The colors indicate Mg–Al spinel-type oxide in cyan Nb-rich particle in yellow, and MnS in purple.

In addition to the targeted Nb-rich particle, the phase map presented in Figure 4 distinguishes other inclusions that are not the target of the automated particle analysis, including an Al–Mg–O inclusion consistent with Mg–Al spinel-type oxide and an Mn–S inclusion with composition consistent with manganese sulfide. These inclusion types are commonly encountered in steels and were separated from the targeted Nb-rich particle population.

ChemiPhase was then used to inspect the surrounding steel matrix at higher magnification. Figure 5 shows two chemically different phases in the steel matrix. The most abundant region is consistent with the Fe-rich steel main matrix, while a second region shows higher apparent carbon content, indicating a carbide-containing constituent. The same map also highlights small Nb-rich particles targeted with Perception Software. Additional fine V-rich particles were also observed. These particles were not included in the current Nb-rich particle-analysis recipe, but they represent a relevant target for future method development aimed at automated detection of nanoscale V-rich carbide candidates.

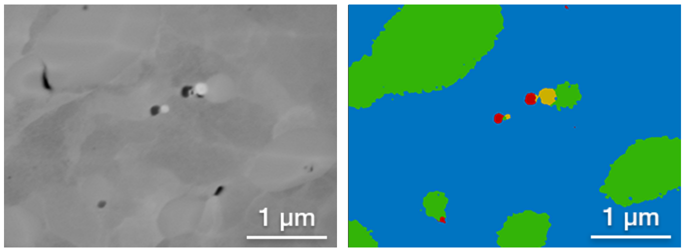

Figure 5. BSE and ChemiPhase images. The map distinguishes two Fe-rich matrix regions in blue and green. Small Nb-rich particles are shown in yellow, while fine V-rich particles shown in red are a focus for future method development.

To complement the composition-based phase mapping, electron backscatter diffraction (EBSD) was used to provide crystallographic phase information for the chemically distinct matrix regions. The EBSD phase map indexed the steel matrix primarily as body-centered cubic (BCC) Fe, with cementite-containing regions also present. This supports the interpretation that the C-enriched Fe-rich regions observed with ChemiSEM Technology correspond to carbide-containing microstructural constituents.

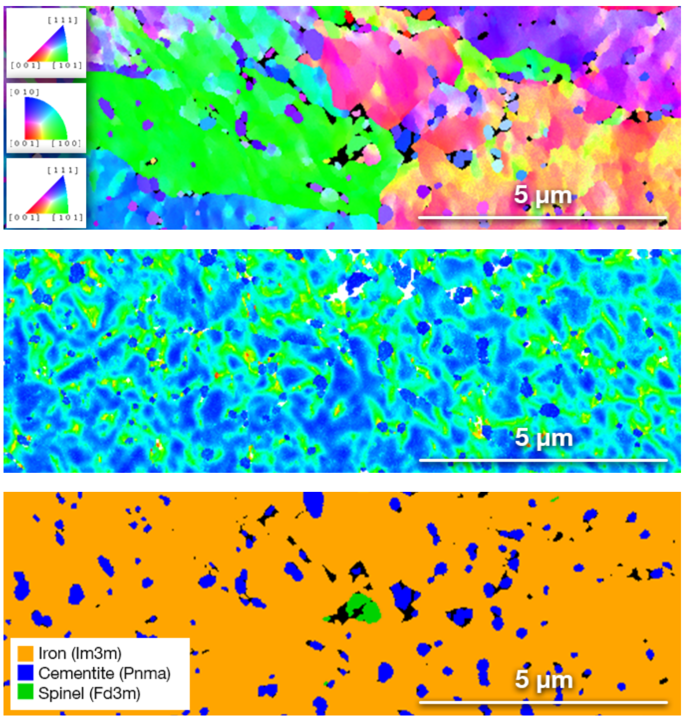

Figure 6. From top to bottom: IPF-Z, KAM, and phase maps.

The inverse pole figure (IPF) in Figure 6 shows a heterogeneous BCC Fe matrix with differently oriented grains and subregions. The kernel average misorientation (KAM) map shows pronounced local misorientation gradients, indicating local lattice distortion consistent with a deformed or processed steel microstructure.

Together, EDS and EBSD complement the automated particle-analysis workflow by providing chemical and crystallographic context. This combined information helps separate the targeted Nb-rich particle population from the surrounding Fe-rich matrix and cementite-containing microstructure.

Conclusions

In microalloyed and HSLA steels, Nb- and V-containing precipitates are important for microstructural control, but their value depends on their size, abundance, and distribution. Because these particles can be very small, routine characterization benefits from combining automated particle analysis with higher-resolution analytical methods.

Perception Software on the Apreo ChemiSEM System enabled traceable automated SEM-EDS particle analysis of the targeted Nb-rich precipitate population. Under the selected 10 kV conditions, the workflow produced a measurable population of classified particles extending into the lower-hundreds-of-nanometers range. ChemiSEM Technology and the TruePix EBSD Detector provided complementary chemical and crystallographic context, helping place the automated particle-analysis results in relation to the surrounding steel microstructure.

Together, the Apreo ChemiSEM System and Perception Software provide a practical workflow for automated, traceable precipitate analysis in microalloyed steel, combining field-emission imaging with chemistry-based particle classification.

Future work will extend the method toward smaller particles, including finer V-rich carbide candidates.

References

Mohrbacher H, Bacchi L, Ischia G, Gialanella S, Tedesco M, D'Aiuto F, Valentini R. Characterization of Nanosized Carbide Precipitates in Multiple Microalloyed Press Hardening Steels. *Metals*. 2023; 13(5):894. https://doi.org/10.3390/met13050894

Sun L, Liu X, Xu X, Lei S, Li H, Zhai Q. Review on niobium application in microalloyed steel[J]. *Journal of Iron and Steel Research International*. 2022; 29(10):1513-1525. http://doi.org/10.1007/s42243-022-00789-1

Learn more at **thermofisher.com/perception**